VACUUM ULTRAVIOLET
LINE RADIATION MEASUREMENTS
OF A SHOCK-HEATED NITROGEN PLASMA

by James O. McClenahan

Ames Research Center
Moffett Field, Calif. 94035

NATIONAL AERONAUTICS AND SPACE ADMINISTRATION • WASHINGTON, D. C. • AUGUST 1972

1. Report No. NASA TN D–6920	2. Government Accession No.	3. Recipient's Catalog No.
4. Title and Subtitle VACUUM ULTRAVIOLET LINE RADIATION MEASUREMENTS OF A SHOCK-HEATED NITROGEN PLASMA		5. Report Date August 1972
		6. Performing Organization Code
7. Author(s) James O. McClenahan		8. Performing Organization Report No. A-4234
		10. Work Unit No. 117-07-04-11-00-21
9. Performing Organization Name and Address NASA Ames Research Center Moffett Field, Calif., 94035		11. Contract or Grant No.
		13. Type of Report and Period Covered Technical Note
12. Sponsoring Agency Name and Address National Aeronautics and Space Administration Washington, D. C. 20546		14. Sponsoring Agency Code

15. Supplementary Notes

16. Abstract

Line radiation, in the wavelength region from 1040 to 2500 Å from nitrogen plasmas, was measured at conditions typical of those produced in the shock layer in front of vehicles entering the earth's atmosphere at superorbital velocities. The radiation was also predicted with a typical radiation transport computer program to determine whether such calculations adequately model plasmas for the conditions tested. The results of the comparison show that the radiant intensities of the lines between 1040 and 1700 Å are actually lower than are predicted by such computer models.

17. Key Words (Suggested by Author(s)) Nitrogen Radiation Ultraviolet Reentry Shock waves	18. Distribution Statement Unclassified – Unlimited		
19. Security Classif. (of this report) Unclassified	20. Security Classif. (of this page) Unclassified	21. No. of Pages 34	22. Price* $3.00

VACUUM ULTRAVIOLET LINE RADIATION MEASUREMENTS OF

A SHOCK-HEATED NITROGEN PLASMA

James O. McClenahan

Ames Research Center

SUMMARY

Line radiation, in the wavelength region from 1040 to 2500 Å from nitrogen plasmas, was measured at conditions typical of those produced in the shock layer in front of vehicles entering the earth's atmosphere at superorbital velocities. The radiation was also predicted with a typical radiation transport computer program to determine whether such calculations adequately model plasmas for the conditions tested. The results of the comparison show that the radiant intensities of the lines between 1040 and 1700 Å are actually lower than are predicted by such computer models.

INTRODUCTION

The state of plasmas produced by a vehicle entering the earth atmosphere at high velocity is shown in figure 1 (ref. 1) for hyperbolic entry. The temperatures produced are such that the radiative heating of a blunt-nosed vehicle by the luminous shock layer is much greater than the convective heating. As the total radiant power incident on the heat shield of a vehicle becomes very large, the spectral character of the radiant flux becomes important because the response of the heat shield surface and ablation products, as well as the self-absorption within the air itself, are functions of the wavelength. The radiation transport from a plasma at conditions typical of earth entry has been studied theoretically by various researchers (refs. 2-6). Calculations may be made using the results of these theoretical studies for continuum and line radiation transport to the heat shield of an entry vehicle. A computer program with which to make such calculations has been developed by Wilson and Grief (ref. 7). This program (RATRAP IV) has been widely used for making reentry heating predictions. The spectral radiance of nitrogen, as calculated by RATRAP IV, for a typical earth atmospheric entry is shown in figure 2.

As noted in figure 2, these calculations show that a very large portion of the radiant energy is transported from the ultraviolet region of the spectrum particularly in atomic lines between 1050 Å and 2000 Å. Unfortunately, the accuracy of the program in this spectral region is uncertain, because the f numbers for atomic radiation in this spectral region are not accurately known (ref. 8).

Two types of experimental measurements of radiation from nitrogen plasmas have a bearing on this problem: (1) arc experiments (refs. 9, 10), and (2) shock-tube experiments (refs. 11, 12). In general, the data obtained from arc experiments are for plasmas that are at the right temperatures but at pressures too high for direct application to reentry cases. The shock-tube data available at these plasma conditions were obtained in the reflected shock mode for which the thermodynamic conditions are not as accurately predictable as would be desirable (ref. 11). Morris, Krey and Garrison

(ref. 9) have obtained arc data in the spectral region of interest here and calculated, from these data, the f number for transitions in this spectral region. These f numbers can be compared to those used in calculations such as those performed by RATRAP IV. Such comparisons are made later in this paper. Shock-tube tests by Marrone, Wurster, and Stratton (ref. 11) were directed at continuum transport in the ultraviolet region. These results show that continuum transport theories, such as used in RATRAP IV, are in agreement with experiment. This work does confirm that the continuum contribution is a small fraction of the total radiation transport in the spectral region of interest at Earth entry conditions. The shock tube tests made by Wood and Wilson (ref. 12) were performed with a broad spectral band and do not provide information about radiation transport over any narrow spectral band, as was of interest here.

The purpose of the work described here was to measure experimentally the spectral radiance of a nitrogen plasma at earth entry conditions. The experiment was performed to determine whether the total radiative energy measurements due to the atomic lines in the region between 1050 Å and 1800 Å agree with available calculations. Further, it was intended that the accuracy of the transition probabilities for those lines used in such calculations would be assessed by this experiment.

The plasmas required for this experiment were produced by means of a shock tube, driven by an electric arc discharge, operated in the incident shock mode, since this facility is capable of very closely duplicating the conditions found in hyperbolic entry. The gas tested was nitrogen because calculations show that this gas is the predominant radiator at earth atmospheric entry conditions.

EXPERIMENTAL EQUIPMENT AND PROCEDURE

The plasma temperature and pressure conditions simulated by use of the arc-driven shock tube are indicated by a horizontal line at 54-km altitude in figure 1. These conditions were obtained behind the incident shock at 8 to 13 km/sec into N_2 at 0.4 torr. The facility has been described in previous publications (ref. 13).

The facility has a 30.47-cm-diameter driven tube approximately 12 m long, which can be evacuated and filled with any desired test gas. The driven tube is connected to a driver chamber, which consists of a 39.4-cm-long by 13.96-cm-diameter chamber separated from the driven tube by a stainless steel diaphragm. The driver chamber is filled with a light gas (for this experiment, a mixture of hydrogen and helium), which is heated by an electric arc. The diaphragm separating the two sections is scribed to an appropriate depth so as to break at a prescribed driver pressure, allowing driver gas to expand into the driven tube and produce a high speed shock wave in the test gas. Properties of the test gas behind the shock may be studied experimentally. Figure 3 is a schematic diagram of the shock tube facility and the equipment used for these tests. Note that although the primary interest of this study was in the vacuum ultraviolet region, a visible radiation detector was also used as a check on the overall experimental and computational procedures, which are less complicated in the visible region. The test gas used in this experiment was ultrahigh-purity nitrogen. The operating procedure and leak rate of this facility were such that the contaminants were less than 0.025 percent (by partial pressure) at the time of firing.

As the shock wave moves down the driven tube, its velocity is measured with ionization gages connected to high frequency counters. The shock velocity and initial test gas pressure are used with

real gas thermodynamic programs to calculate the equilibrium conditions behind the shock. Splitter plates are used to isolate a portion of the shock heated gas, free of side-wall boundary layers. The shock wave is observed with radiation detectors whose fields of view are established by collimation slits separated by 30.47 cm. To obtain radiation signals with adequate fidelity, it is necessary that the field of view of the collimation system be small with respect to the shock layer thickness. In addition the electronic rise time must be short enough to be negligible with respect to the variation in the signals from the detectors themselves. The signals were measured and recorded by use of oscilloscopes with polaroid camera attachments. The sum of the geometric time resolution and the electronic rise time was less than 1 μsec for this experiment. Ionization gages were used to trigger the oscilloscopes before the shock arrived in the field of view of the detector system so that the entire history of radiation could be observed. Figure 4 shows typical data obtained in this experiment; the sudden downward deflections in the oscilloscope traces correspond to the arrival of the incident shock. The relatively uniform region following corresponds to the "clean" layer of shock heated test gas. The fact that the signal does not change appreciably during this time is evidence that the plasma is at thermodynamic equilibrium. The end of this region marks the arrival of the driver gas interface into the field of view of the instruments.

The spectral dependence of the response was determined from the spectral response of the photocathodes and spectral transmission of the various windows used. The overall spectral characteristics with each type of window used are shown in figure 5. The location of the line group centers from the RATRAP IV output code in the spectral region of interest is shown; the numbers are those used in the RATRAP IV code. Figure 6 shows the RATRAP IV output for the same conditions as in figure 4, but with the coordinates transformed to wavelength units such that the effect of filter functions may be more easily visualized. Examination of figures 5 and 6 shows how the relative contribution of these line groups to the output signal of the detector system is changed by the use of different windows, thus the contribution from the several line groups could be determined even though the system itself is of relatively broad spectral sensitivity. Table 1 shows the relative effect on the output radiometer signal of radiation from the various line groups, as calculated by RATRAP IV, for the different window combinations used in this experiment.

TABLE 1.– SPECTRAL CONTRIBUTIONS TO RADIOMETER SIGNAL

[Shock tube conditions: 0.4 torr initial pressure, 10 km/sec. Total radiative power: 23.11 W/cm^2-sr. Ultraviolet detector system.]

Window type	Spectral range	Wavelength, Å						
		$\leqslant$1169	1227	1305	1409	1540	1710	Continuum
LiF	1040–2500	3.168	8.20	4.57	3.53	42.1	29.9	8.45
LiF+MgF$_2$	1130–2500	1.472	5.10	3.23	3.11	44.4	33.97	8.68
CaF$_2$	1220–2500	0	4.55	5.365	4.003	45.4	31.6	9.19
CaF$_2$+Al$_2$O$_3$	1450–2500	0	0	0	0	41.56	45.1	13.3
SiO$_2$	1550–2500	0	0	0	0	0	75.6	24.4

Visible detector system

		3493	4350	6703	8267	Continuum
SiO$_2$	3000–8000	7.20	10.29	5.56	.45	76.5

To obtain quantitative results, it was necessary to measure the spectral response of the detectors and the spectral transmission of each window used in this experiment. This is a difficult undertaking under the best of conditions, but for the ultraviolet region from 1000 to 2500 Å it is more difficult because the calibrations must be done in a vacuum, there are no calibrated hot filament lamps, discharge lamps radiate at very minute levels, and monochrometers have poor efficiencies. A valuable reference for use in such work is Samson (ref. 14). The calibrations required for this experiment were in the region from 1050 Å to 2500 Å for the ultraviolet detector and in the region from 3000 Å to 8000 Å for the visible detector. The ultraviolet detector was calibrated as follows (ref. 15):

1. *Calibration between 1050 Å and 1800 Å.* A photomultiplier sensitive to visible radiation was made sensitive to vacuum ultraviolet radiation by means of a sodium salicylate coated window. This broadband detector was calibrated with respect to a xenon-filled ionization chamber, an accepted standard between 972 Å and 1022 Å. Then this detector (assumed to be spectrally flat) was used as a secondary standard to calibrate the visibly blind ultraviolet detector at various discrete wavelengths between 1050 Å and 1800 Å. The radiation for this procedure was obtained by means of a 0.5-m Jerrall-Ash monochrometer with an 800-Å blaze concave grating. A capillary tube discharge lamp using H_2 gas was used as a light source. The input and output of the monochrometer were differentially pumped. The window transmission curves were measured using this setup for the wavelength region of 1040 Å to 1700 Å. For longer wavelengths, the window spectral transmissions were measured with a Beckman DK2 spectrophotometer.

2. *Calibration at 1470 Å.* A xenon-filled lamp that radiates over 90 percent of its total energy at 1470 Å and whose output was factory calibrated to ±50 percent was used as a double check of the calibration performed in step 1. The detector sensitivity obtained here agreed quite closely with that obtained in step 1 (near 1470 Å).

3. *Calibration at 2537 Å.* A thermocouple was calibrated with respect to a standard tungsten iodine 1000-W lamp, which was traceable to NBS black-body standards to an accuracy of ±15 percent. The thermocouple was then used to measure the output of a mercury arc lamp through a 0.25-m Bosch and Lomb monochrometer at 2537 Å. The ultraviolet detector was then calibrated with this source of radiation. This test was important to verify that the detector was insensitive at $\lambda > 2000$ Å.

The visible calibration was done by means of a 1000-W tungsten iodine lamp (GE Type DWX-1000) calibrated by Epply Laboratory, Inc. It was used as the standard for calibration of the visible response photomultiplier over its spectral range.

THEORETICAL PREDICTION

For a given combination of spectral sensitivity and window transmission, the measured signal may be described by

$$V = \frac{A_1 A_2}{r^2} RK_E K_I \int_O^\infty I_\lambda K_\lambda W_\lambda \, d\lambda \qquad (1)$$

where

V the voltage measured at the output of the photomultiplier

A_1, A_2 optical collimation slit areas

r separation between optical collimation slits

R load resistance

K_E photomultiplier gain

K_I current gain of external preamplifier, if used

I_λ spectral radiance of the plasma

K_λ spectral sensitivity of photocathode

W_λ spectral transmission of window

All the terms in equation (1) may be measured except I_λ, the spectral shape of which must be known for evaluation of the integral. The experiment yields V, but there are infinitely many solutions for I_λ that would satisfy the expression for any given V. Therefore, some prior information relative to the spectral shape of I_λ is required before the measured data may be interpreted. If a given spectral shape for I_λ is assumed, the integral may be evaluated and the absolute magnitude of the assumed I_λ is given uniquely by the observed value of V.

A literature search to find the spectral shape for I_λ showed that much work has yet to be done in this area. At the temperatures and pressures required, the gas is highly ionized and tends to radiate strongly in the ultraviolet region of the electromagnetic spectrum. The f numbers for transitions in the ultraviolet are not accurately known. The NBS tables (ref. 8) for atomic nitrogen lines are given with an accuracy rating of D^- which indicates an accuracy worse than ±50 percent.

The RATRAP IV program was used in obtaining both the relative spectral shape and the amplitude of I_λ. The f numbers for the most part are from the NBS tables, although experimental results were used where available (ref. 7). The inputs to this program are path length, temperature, and pressure. The output was the spectral radiance for a slab of gas, in local thermodynamic equilibrium, of infinite extent in the axis normal to the direction of radiation transport and of the appropriate thickness. Since the shock tube test section between the splitter plates is of rectangular cross section and the actual optical field of view is small, the geometry of the experiment has been assumed to simulate this configuration adequately. The infinite slab assumption has been studied (ref. 16) and has been found to be valid over the range of conditions tested here (although it tends to produce error at higher temperatures than those of interest here due to radiative cooling).

The output of the RATRAP IV program in the spectral region of interest cannot be compared directly to any existing data. The output of the program contains continuum radiation. The continuum edge located near 1100 Å (fig. 6) has been studied experimentally by Morris, Krey and Garrison (ref. 9) and by Marrone, Wurster and Stratton (ref. 11). Their data confirm that this edge

is located as predicted by RATRAP IV. This agreement between experiment and the theoretical prediction used is evidence that the continuum contribution to radiation between 1050 Å and 2000 Å is small. The output of the program also contains atomic line radiation. The f numbers obtained in arc experiments by Morris, Krey, and Garrison (ref. 9) and Labuhn (ref. 10) may be compared to those used in RATRAP IV for many of the lines in the spectral region of interest; such a comparison indicates agreement to better than a factor of 2 for all line groups, except that the f number used by RATRAP IV for the line group at 1710 Å appears to be too low by a factor of ~5.

The temperature and pressure for a given set of shock tube conditions was next determined by use of the method outlined in Chapter VI of Vincenti and Kruger (ref. 17). Because of the large temperature dependence of ultraviolet radiation, these thermodynamic calculations are very important. The temperature and pressure found behind the shock wave were later calculated independently by use of a computer program developed at JPL (ref. 18) and found to agree to within a few percent.

The experimental data may then be further reduced by utilizing the I_λ from the RATRAP IV program for conditions found as described above. The experimentally measured value of $\int_0^\infty I_\lambda K_\lambda W_\lambda \, d\lambda$ then may be compared to the computed value and the $\int_0^\infty I_\lambda \, d\lambda$ found from

$$\int_0^\infty I_\lambda \, d\lambda = \left[\int_0^\infty I_{\lambda(\text{RATRAP IV})} \, d\lambda \right] \frac{\int_0^\infty I_\lambda K_\lambda W_\lambda \, d\lambda}{\int_0^\infty I_{\lambda(\text{RATRAP IV})} K_\lambda W_\lambda \, d\lambda} \tag{2}$$

This expression is valid for the wavelength region in which the measurements are made and depends on the assumption that the spectral shape of the radiant intensity is as predicted by the RATRAP IV program.

RESULTS AND DISCUSSION

The results of this experiment are shown in figures 7 through 15. Note that the parameter of comparison between the theory and the experimental results is $\int_0^\infty I_\lambda K_\lambda W_\lambda \, d\lambda$, which was discussed in the preceding section. The theoretical curve on these plots is shown as a double line. The RATRAP IV program has its line intensity calculations based on f numbers that are not accurately known. The theoretical curves were developed by changing the f numbers used in the program by ±50 percent. The variation in radiative intensity corresponding to this change in f number is small because the plasma is optically thick at the line centers in this spectral region.

The data points plotted on these curves are proportional to the radiant intensity in the wavelength region in which the window transmits light and for which the photocathode itself is sensitive. The photomultiplier signal is given by

$$i \propto \int_0^\infty I_{\lambda \text{continuum}} K_\lambda W_\lambda \, d\lambda + \sum_n I_n K_n W_n \quad \text{for } n = 1 \text{, all lines} \tag{3}$$

This expression may be studied to determine the effectiveness of radiation to produce a signal at the photomultiplier as a function of the wavelength. The contributions to the signal of the various sources of radiation for the various windows used in this experiment are summarized in Table 1. This table is to be interpreted as follows: the first column gives the window type; the second column gives the spectral range in which the combination of detector and window is sensitive; and subsequent columns give contributions to the signal current in percentage of the total signal current available from the detector. The visible radiometer system is presented analogously.

The data plots of figures 7 through 15 indicate disagreement between RATRAP IV predictions and the measurements between 1040 and 1500 Å, especially at the highest velocities. Since the data scatter is large, it is not possible to make any immediate judgements about the f numbers used in the program, but, in general, the RATRAP IV calculations predict more radiation in the region between 1040 and 1500 Å than was measured during this experiment.

The error in the data points due to error in the measurement of velocity is less than 1 percent. The measurements of sensitivity of the photomultipliers, the window transmission curves, and the other constants have been analyzed and found to have an accuracy of better than ±40 percent. The data scatter obtained in this experiment is greater than ±40 percent and thus governs the confidence that may be placed with a given data measurement. Study of the devices used in this experiment indicates that the data scatter does not depend on variations in the equipment used to perform the measurement but rather depends on the variations in the conditions found in the test gas itself. The conditions found behind the incident shock are calculated from the shock-wave velocity and the initial conditions in the undisturbed test gas.

The radiant intensity of a plasma is very sensitive to temperature; if the temperature produced varies from shot to shot, it would be expected that such data would be scattered. The shock wave is developed in a shock tube by means of a "piston" made of a light gas, rather than a solid. The interface shape between the test gas and this piston varies markedly in shape from shot to shot. The effect of this variation, if any, on the shock-wave temperature is not known. The data are assumed, therefore, to be randomly scattered and a statistical average taken over as many shots as possible is the best method of analysis of this type of data.

When analyzed with an averaging technique, discussed in detail below, the data tend to be lower than the theory except for two cases: (1) for the suprasil data taken in the ultraviolet region (fig. 14), and (2) for the visible data at velocities below about 10 km/sec (fig. 15). The visible data obtained here agree well at high velocities but are above the theory at low velocities. At high temperatures, the radiation of gases tends to be dominated by atomic radiation, while at low temperatures it is dominated by molecular radiation. The RATRAP IV program is intended for use at high temperatures and therefore neglects molecular radiation. This experiment shows that for the simulated conditions, a radiation transport program that ignores molecular radiation is inadequate in the visible region at the lower velocities. Another prediction of radiation from nitrogen plasmas in use at Ames Research Center was used in checking the results in the visible region. This prediction was obtained by means of a computer program developed by Whiting, Arnold, and Lyle (ref. 19) which was run for the atomic lines only and found to agree quite closely with the RATRAP IV output. Molecular radiation was included next, and it was found to increase the prediction at the lower velocities (fig. 15). The measured data at the lowest velocities agree quite closely with the theoretical prediction. For the suprasil data, the measured data were higher than the prediction at the low velocities; unfortunately, only one point is available and no conclusion may be drawn, but it is possible that the

7

RATRAP IV prediction could be low at the lower velocities for this spectral region for the same reason as for the visible region since the signal is due primarily to continuum (see table 1). The prediction of Whiting, Arnold and Lyle (ref. 19) shows molecular radiation down to 2600 Å, this could possibly affect the signal for the system using the suprasil window. Detailed investigation of this point has not been carried out because of the lack of data.

The final results are presented in the velocity profiles of figures 16 through 20, which are similar to those of figures 7 through 15 except that the coordinates have been transformed to photometric units, by means of equation (2), for purposes of general utility. The theoretical prediction of radiant power from the RATRAP IV program, shown as a solid line, is

$$P = \int_{\lambda_1}^{\lambda_2} I_\lambda \, d\lambda \tag{4}$$

The dashed line is the least-squares fit of the data obtained in the spectral region of interest. In figures 16 through 18, the slope of the dashed line is chosen to be equal to the slope of the theoretical prediction, and its position was determined from:

$$\log I_{\text{int}} = \frac{1}{m} \sum_{n=1}^{m} (\log I_n - av_n) \tag{5}$$

where

I_{int} intensity intercept of the dashed line

I_n intensity of the nth data point

V_n velocity of the nth data point

m number of points

a slope of the theoretical prediction

When the one data point below 10 km/sec is ignored the dashed line falls right on the solid line denoting the theoretical prediction, as shown in figure 19. It is unfortunate that more data were not obtained here, but after an exhaustive search for a definite source of excess signal at this set of conditions it was concluded that this data point should probably be ignored. The final curve (fig. 20) is for the visible data. Again, the data were reduced to a single line by the method used previously except that the slope of the line was taken from the Whiting program (ref. 19). In figure 20 the two solid lines represent predictions made by each of the programs. It should be noted that the Whiting, Arnold and Lyle program output for atomic lines only agrees quite closely with that of the RATRAP IV program. This is to be expected since the spectral region of interest here is at a wavelength at which the radiation characteristics of the gas are well known.

The ultraviolet plots of figures 16 through 19 show a marked increase in error with bandwidth. The radiation is overpredicted by a factor of 3 for the lithium fluoride region. The disagreement progressively decreases with the spectral interval until no appreciable discrepancy is found for the suprasil region. To facilitate the efficient computation of the large number of lines involved in a given case, the RATRAP IV applies a "grouping" technique in which various multiplets are grouped

8

together and an appropriate f number used such that the total intensity calculation will be accurate. Because of this program characteristic, and since the multiplets themselves already constitute a group of lines, it is necessary to determine that the effect of moving lines to the wrong wavelength will not cause an error, especially when the spectrum is to be used with narrowband spectral sensitivity and filter functions. In the region of interest, 1040 to 2500 Å, there are about 100 lines calculated in the program. These lines are lumped together into six groups at separate wavelengths. This grouping of lines is necessary for economy of computing (see ref. 2). The criteria used for the grouping of lines are: (1) in the wavelength interval over which the grouping is done, there must be no absorption edges in the continuum, and (2) the Planck function must not vary significantly with wavelength. The region in which these criteria are most easily met is in the red end of the spectrum; therefore, it is here that the lines are grouped together from a wider wavelength displacement. When used with spectral sensitivity and filter functions, the program is less likely to produce error in the ultraviolet region since the lines cannot be grouped from such a wide wavelength displacement.

In the ultraviolet region of interest, the location of the lines was studied, and it was concluded that a negligible error was produced by the grouping of lines. The next step is to examine the data (figs. 16 through 20) to determine which line groups contain the overprediction. From table 1, it may be seen that: (1) the suprasil data were predicted accurately, and therefore the continuum and the line group at 1710 Å are predicted accurately; (2) the calcium fluoride plus sapphire region is predicted about 30 percent too high, therefore almost no radiation is being produced by the line group at 1540 Å; (3) the calcium fluoride region is predicted too high by about a factor of 2, and if the signal due to the line group at 1540 Å were removed, the theory would be consistent with the data; and (4) the lithium fluoride prediction is too high by about a factor of 3, and although removal of the 1540 Å line group would not lower the prediction sufficiently, removal of all the line groups below 1540 Å plus the 1540 Å line group would make the theory consistent with the data. A statistical analysis (appendix) of the data was performed to confirm that their precision was sufficient for conclusions about these results to be formulated. The analysis results indicate that both accuracy and precision are on the order of ±50 percent or less; therefore, the inconsistency between the experiment and the theory is real and not introduced by the measurements themselves.

The conclusion that the lines do not contribute as much radiation as predicted by the theory is very disturbing and suggests the need for either a re-examination of the way the lines are transported in the RATRAP IV program or an experiment directed at these line groups, with a higher spectral resolution than was employed here.

CONCLUDING REMARKS

The data indicate that the RATRAP IV prediction of line radiation is too high in the ultraviolet region between 1040 and 1550 Å. The RATRAP IV prediction is adequate in the visible region between 3000 and 8000 Å at high entry shock velocities, but it is too low at lower shock velocities because it does not include molecular radiation.

Ames Research Center
National Aeronautics and Space Administration
Moffett Field, California 94035, May 16, 1972

APPENDIX A

DATA PRECISION ANALYSIS

To obtain a measure of the experimental precision achieved in the work described, a brief statistical analysis of the data was carried out as follows. Let

$$\gamma_n(v) \equiv |\bar{I}_n(v) - I_n(v)| \tag{A1}$$

where

$\gamma_n(v)$ discrepancy between the mean of all measured signals and the actual value of the nth measurements at the measured velocity

$\bar{I}_n(v)$ value of mean at the velocity corresponding to the nth data point

$I_n(v)$ actual value of nth data point

A statistic that can be used to characterize the precision of the data is the mean relative error — that is, the ratio (γ_n/I_n), which was computed from

$$\frac{\gamma_n}{I_n} = \frac{1}{K} \sum_{n=1}^{K} \left| \frac{\gamma_n(v)}{I_n(v)} \right| \tag{A2}$$

These statistics are tabulated in table 2. Because the discrepancy between the experimental data and the theory is much larger than can be explained by experimental precision or accuracy, it can be concluded that the discrepancy is real.

TABLE 2.–PERCENTAGE PRECISION IN EXPERIMENTAL DATA

Spectral region, Å	Statistical variation in data, percent
1040–2500	±53.5
1130–2500	±55.6
1220–2500	±53.9
1450–2500	±51.0
1550–2500	±70.6*

*Two points used.

REFERENCES

1. Berggren, Robert E.; Compton, Dale L.; Canning, Thomas N.; Page, William A.: Ames' High-Explosive Shock-Tube Facility. 7th International Shock Tube Symposium, Toronto, Canada, June 23-25, 1969.

2. Hahne, Gerhard E.: The Vacuum Ultraviolet Radiation from N^+-and O^+-Electron Recombination in High Temperature Air. NASA TN D-2794, 1965.

3. Sherman, M. P.; and Kulander, J. L.: Free-Bound Radiation from Nitrogen, Oxygen, and Air. General Electric Corp. R65SD15, May 1965.

4. Vorobyov, V. S.; and Norman, G. E.: Energy Radiated in Spectral Lines by an Equilibrium Plasma. II. Opt. Spectry., vol. 17, no. 2, Aug. 1964, pp. 96-101.

5. Hunt, Brian L.; and Sibulkin, Merwin: Radiative Transfer in a Gas of Uniform Properties in Local Thermodynamic Equilibrium. Part 3: A Detailed Calculation for Nitrogen. Rep. Nonr-562(35)/18, Div. of Engr., Brown Univ., Dec. 1966.

6. Wilson, K. H.; and Nicolet, W. E.: Spectral Absorption Coefficients of Carbon, Nitrogen, and Oxygen Atoms. NASA CR-73049, 1966.

7. Wilson, K. H.; and Grief, R.: Radiation Transport in Atomic Plasmas. Lockheed Missiles and Space Co., Rep. 6-77-67-31, Nov. 1967.

8. Wiese, W. L.; Smith, M. W.; and Glennon, B. M.: Atomic Transition Probabilities. NBS Rep. NSRDS-NBS 4, 20 May 1966.

9. Morris, J. C.; Krey, R. U.; and Garrison, R. L.: Radiation Studies of Arc Heated Nitrogen, Oxygen, and Argon Plasmas. Rep. No. AVssD-0049-68-RR, Space Syst. Div., AVCO Corp., March 1968.

10. Labuhn, Franz: Messung der Absorptionsoszellatorenstärken von NI-Myltiplets am Kashadenlichtbogen un Wellenlängenbereich zwischen 1000 and 1800 Å Z Naturforsch. 20a, 1965, pp. 998-1010.

11. Marrone, Paul V.; Wurster, Walter H., Stratton, John E.: Shock Tube Studies of N^+ and O^+ Recombination Radiation in the Vacuum Ultraviolet. NASA CR-96235, 1968.

12. Wood, Allen D.; and Wilson, Kenneth H.: Radiant Energy Transfer Measurements in Air. NASA CR-1390, 1969.

13. Presley, L. L.; Falkenthal, G. E.; Naff, J. T.: A One MJ Arc Discharge Shock Tube. Proc. 5th Int. Shock Tube Symp. April 28-30, 1965, June 1966, pp. 857-878.

14. Samson, James A. R.: Techniques of Vacuum Ultraviolet Spectroscopy. John Wiley and Sons, Inc., New York, 1967.

15. McClenahan, J. O.: Calibration of Radiation Detectors in the Wave-Length Region Between 972-2500 Å. NASA TN D-   , 1972.

16. Chien, Kuei-Yuan; and Compton, Dale L.: Radiative Cooling of Shock-Heated Air in Cylindrical Shock Tubes. AIAA J., vol. 8, no. 10, Oct. 1970, pp. 1896-1898.

17. Vincenti, Walter G.; and Kruger, Charles H., Jr.: Introduction to Physical Gas Dynamics. John Wiley and Sons, Inc., 1965.

18. Horton, T. E.; and Menard, W. A.: A Program for Computing Shock-Tube Gasdynamic Properties. NASA CR-99337, 1969.

19. Whiting, E. E.; Arnold, J. O.; and Lyle, G. C.: A Computer Program for a Line-By-Line Calculation of Spectra From Diatomic Molecules and Atoms Assuming a Voigt Line Profile. NASA TN D-5088, 1969.
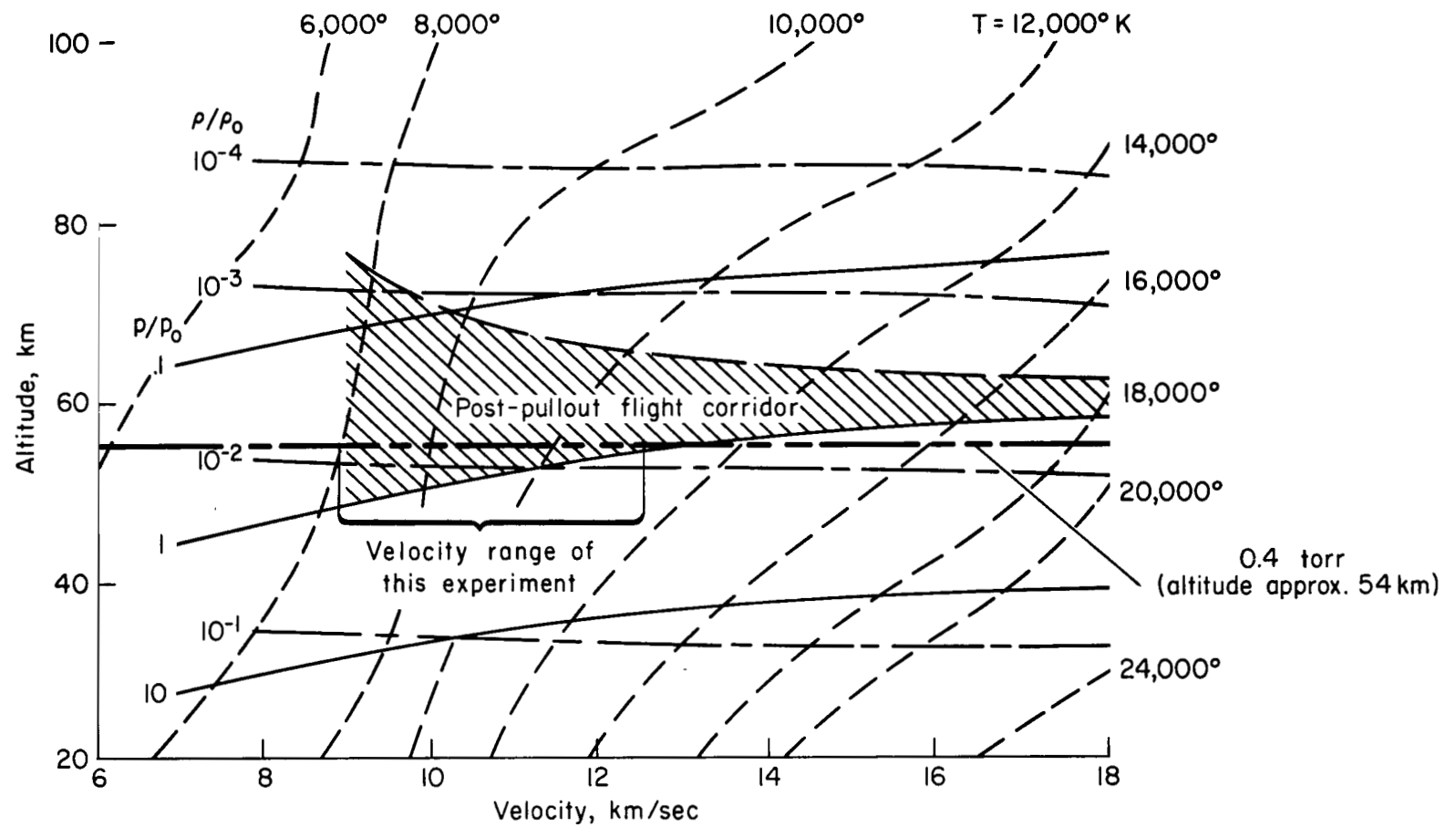
Figure 1.—Thermodynamic properties of plasma produced in shock layer ahead of typical earth entry vehicle (see ref. 1).
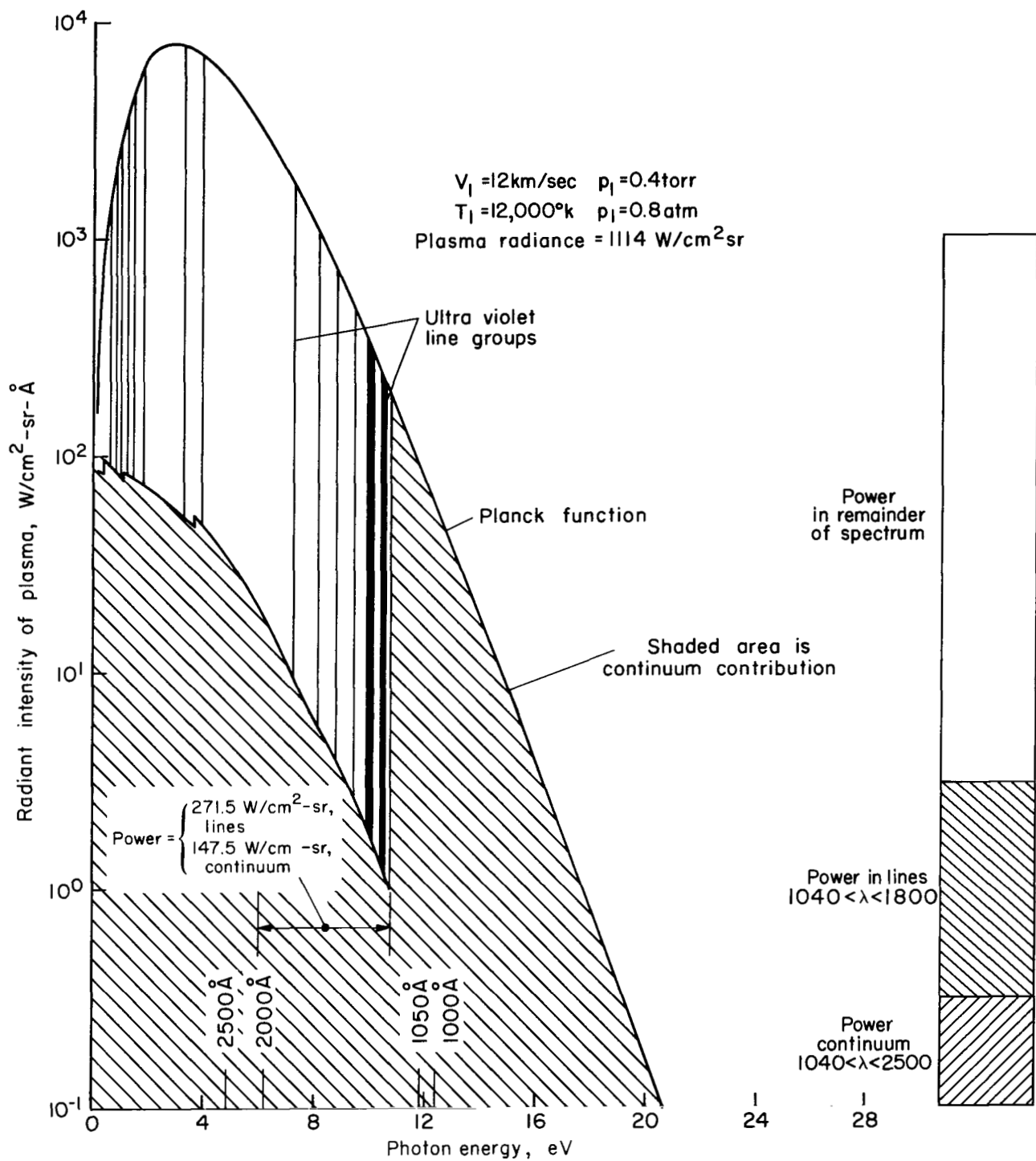
Figure 2.–Spectral radiance produced by nitrogen plasma.

14
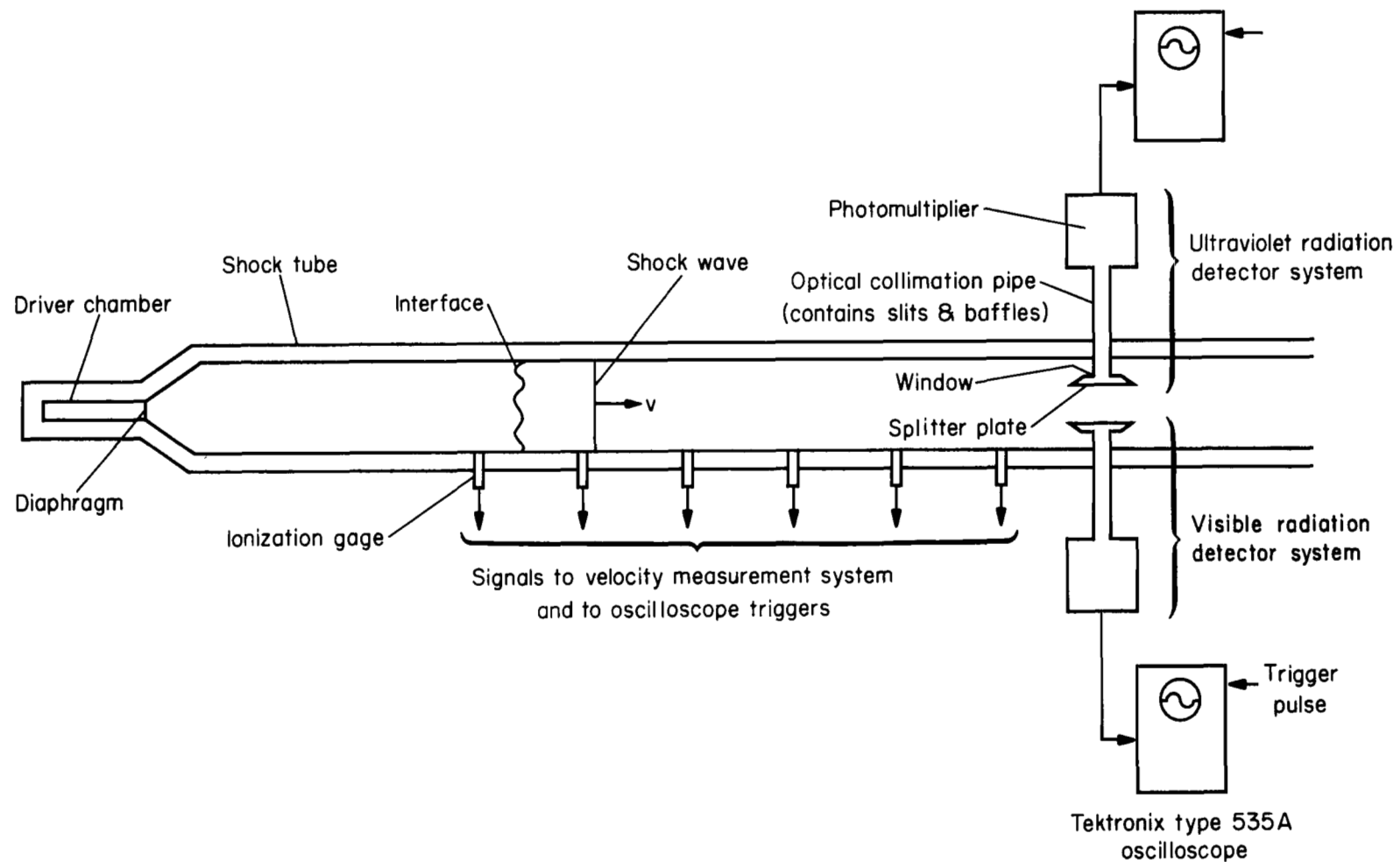
Figure 3.–Experimental setup.
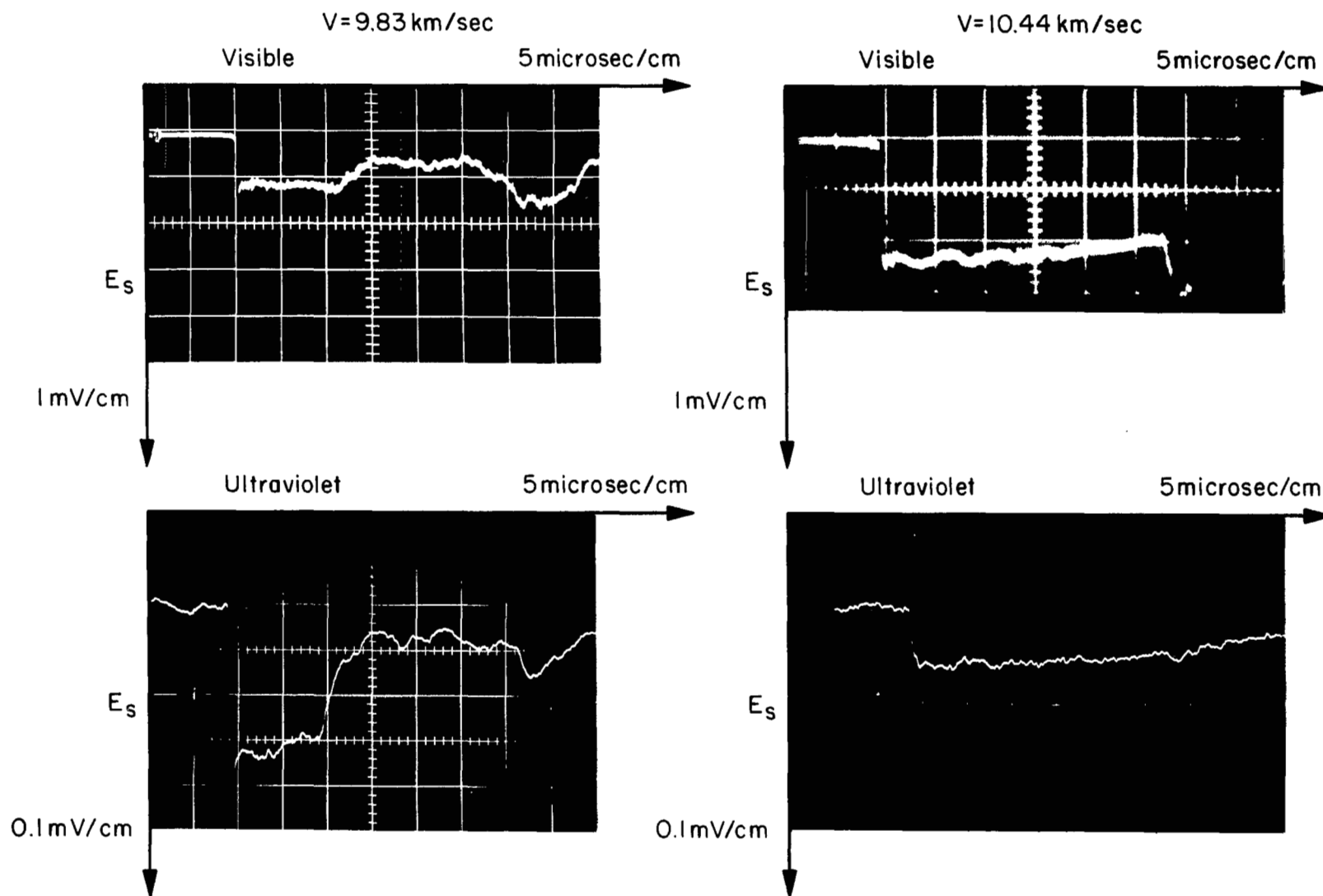
Figure 4.—Typical data.
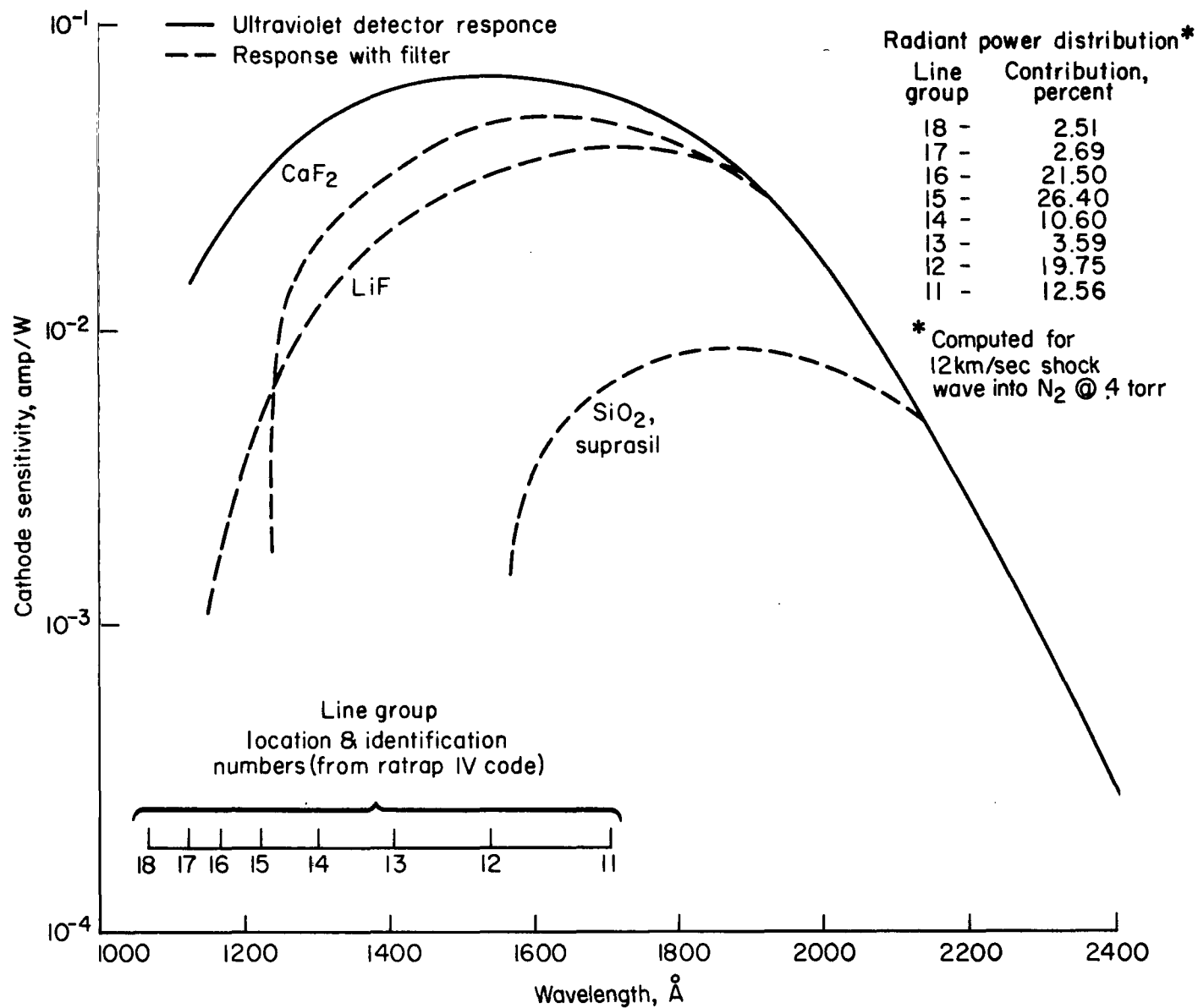
Figure 5.—Ultraviolet detector system — spectral sensitivity.
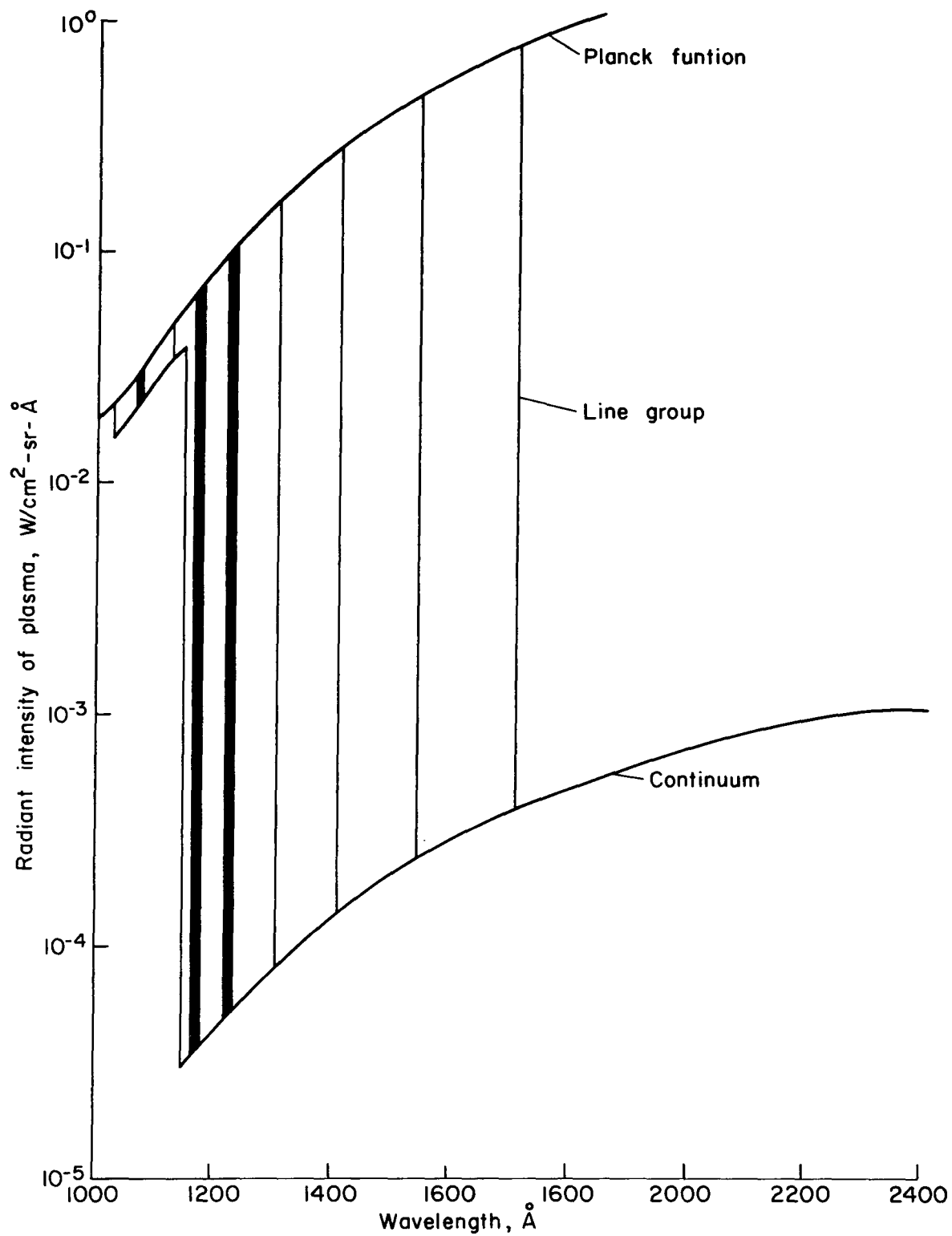
Figure 6.—RATRAP IV output for 10 km/sec shock wave into N_2 at 0.4 torr and 30 cm path length.
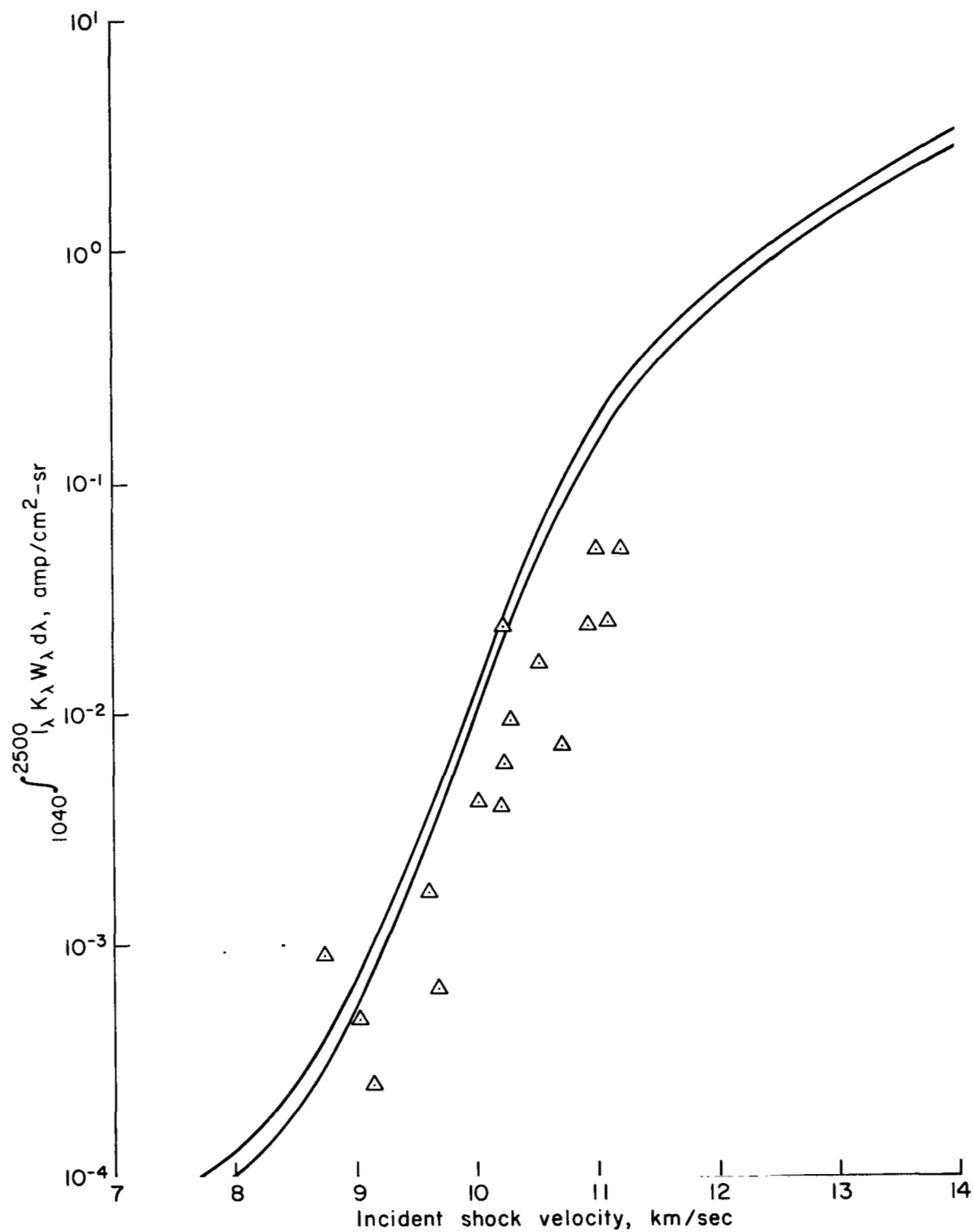
Figure 7.—Data obtained with lithium fluoride window, spectral range 1040-2500 Å.
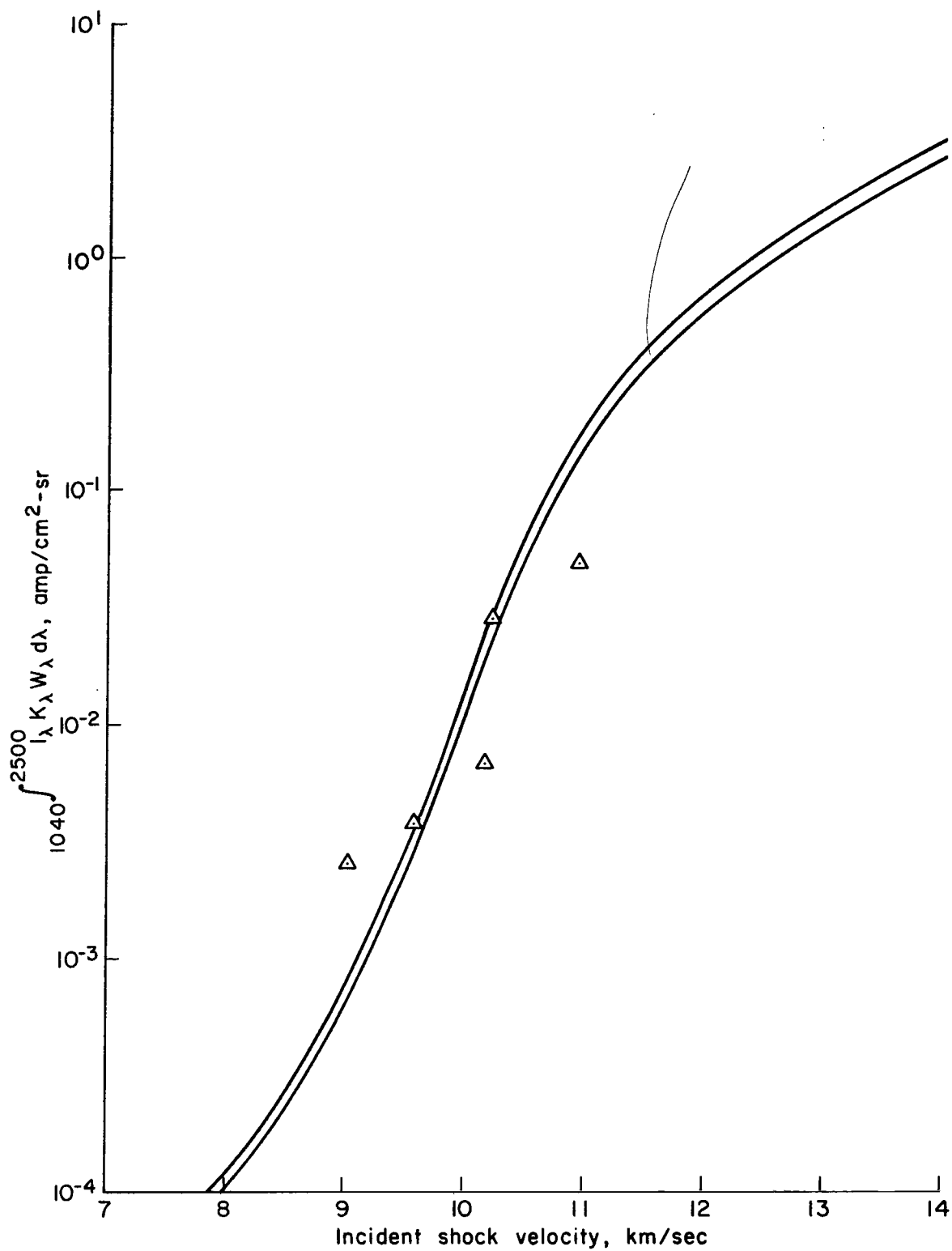
Figure 8.—Data obtained with second lithium fluoride spectral range 1040-2500 Å.
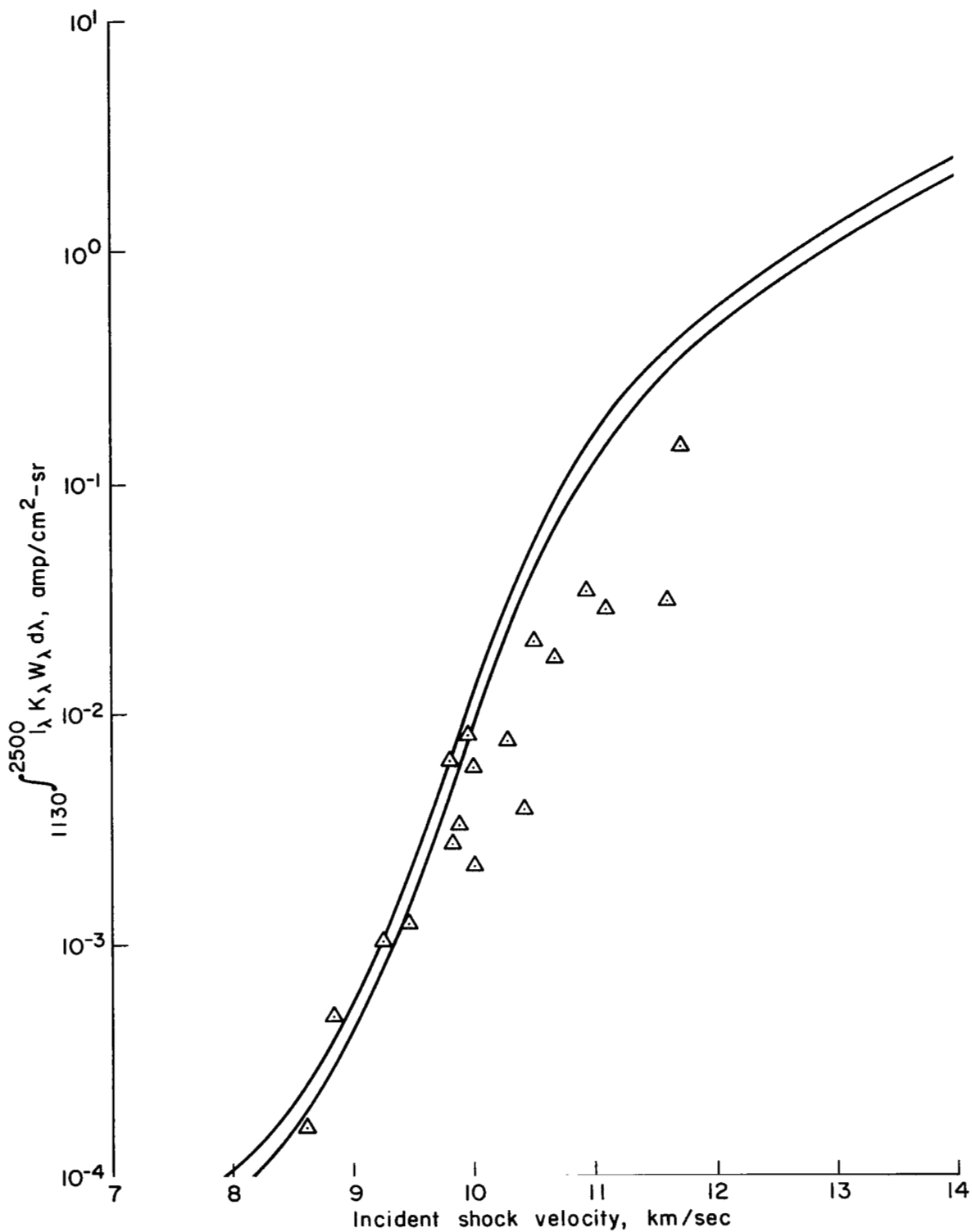
Figure 9.—Data obtained with lithium fluoride plus magnesium fluoride window combination, spectral range 1130-2500 Å.
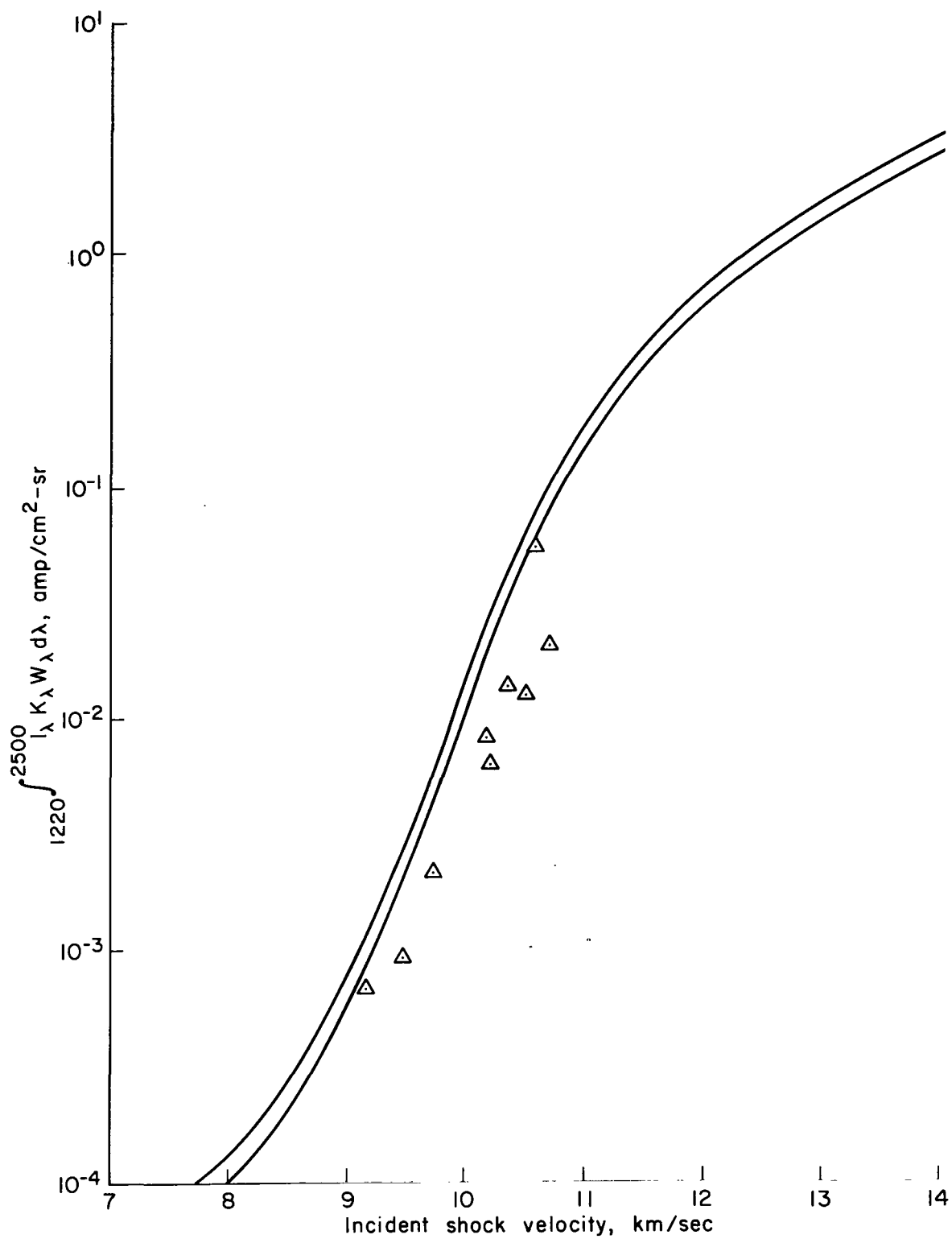
Figure 10.—Data obtained with calcium fluoride window, spectral range 1220-2500 Å.
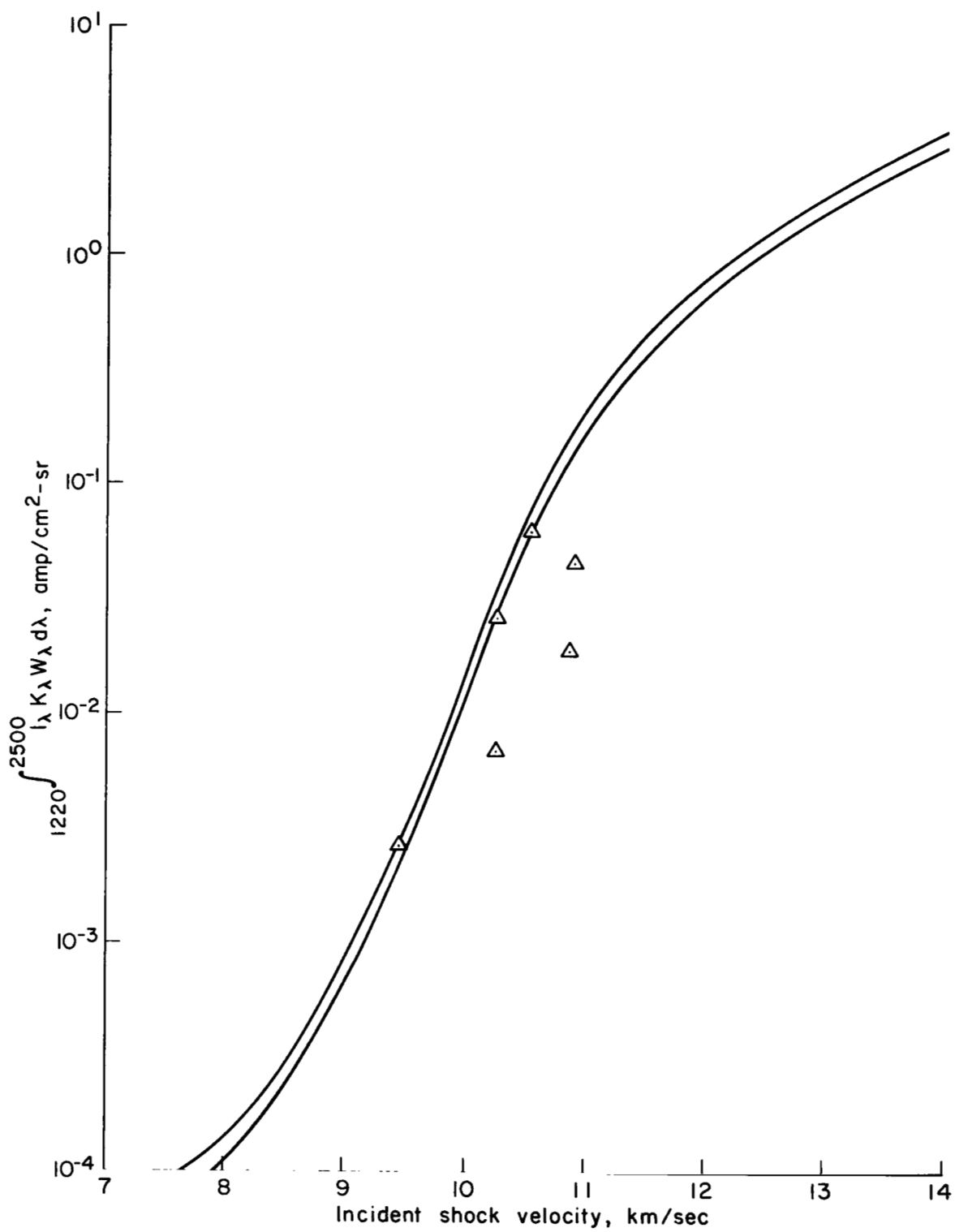
Figure 11.—Data obtained with second calcium fluoride window, spectral range 1220-2500 Å.
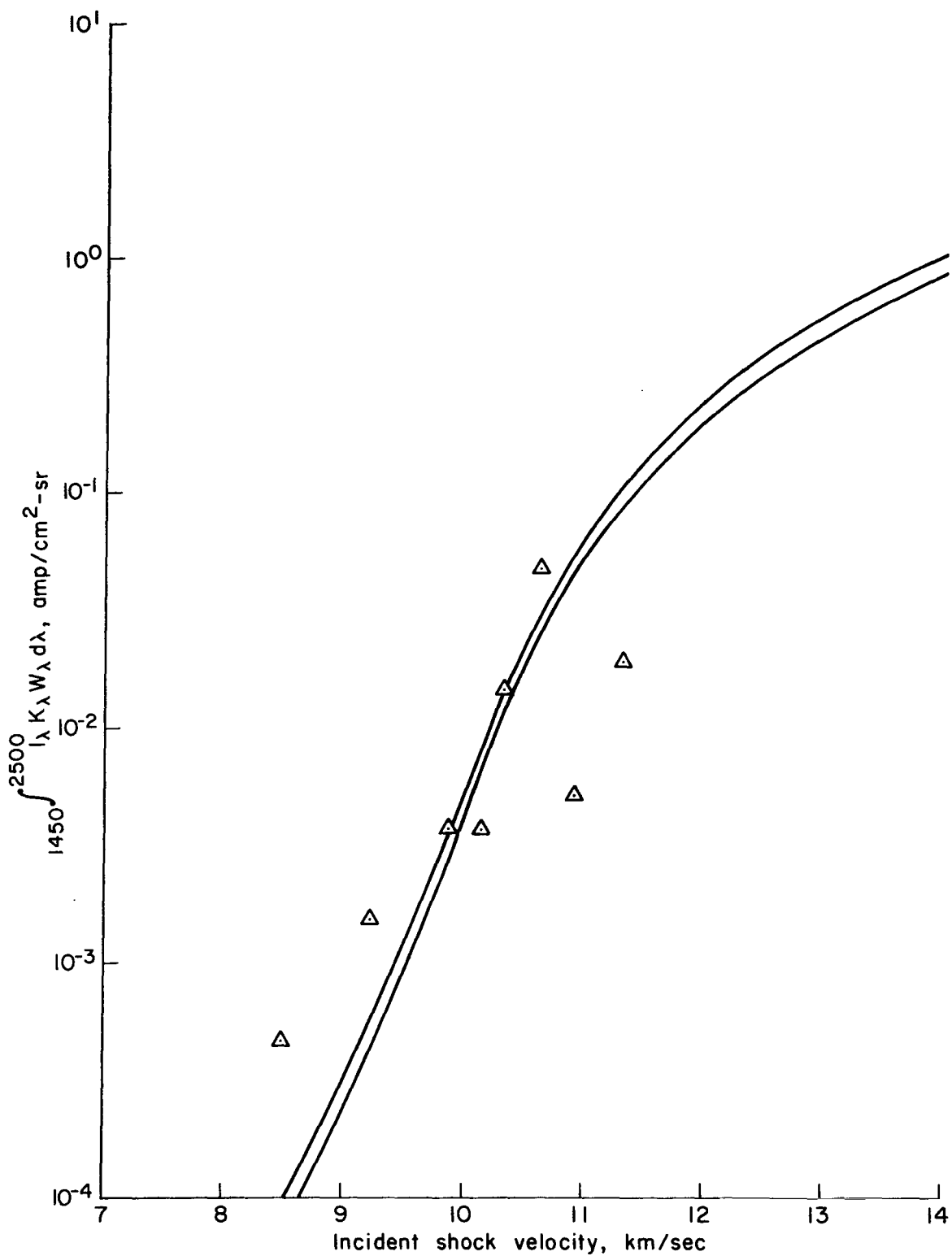
Figure 12.–Data obtained with calcium fluoride plus sapphire window combination, spectral range 1450-2500 Å.
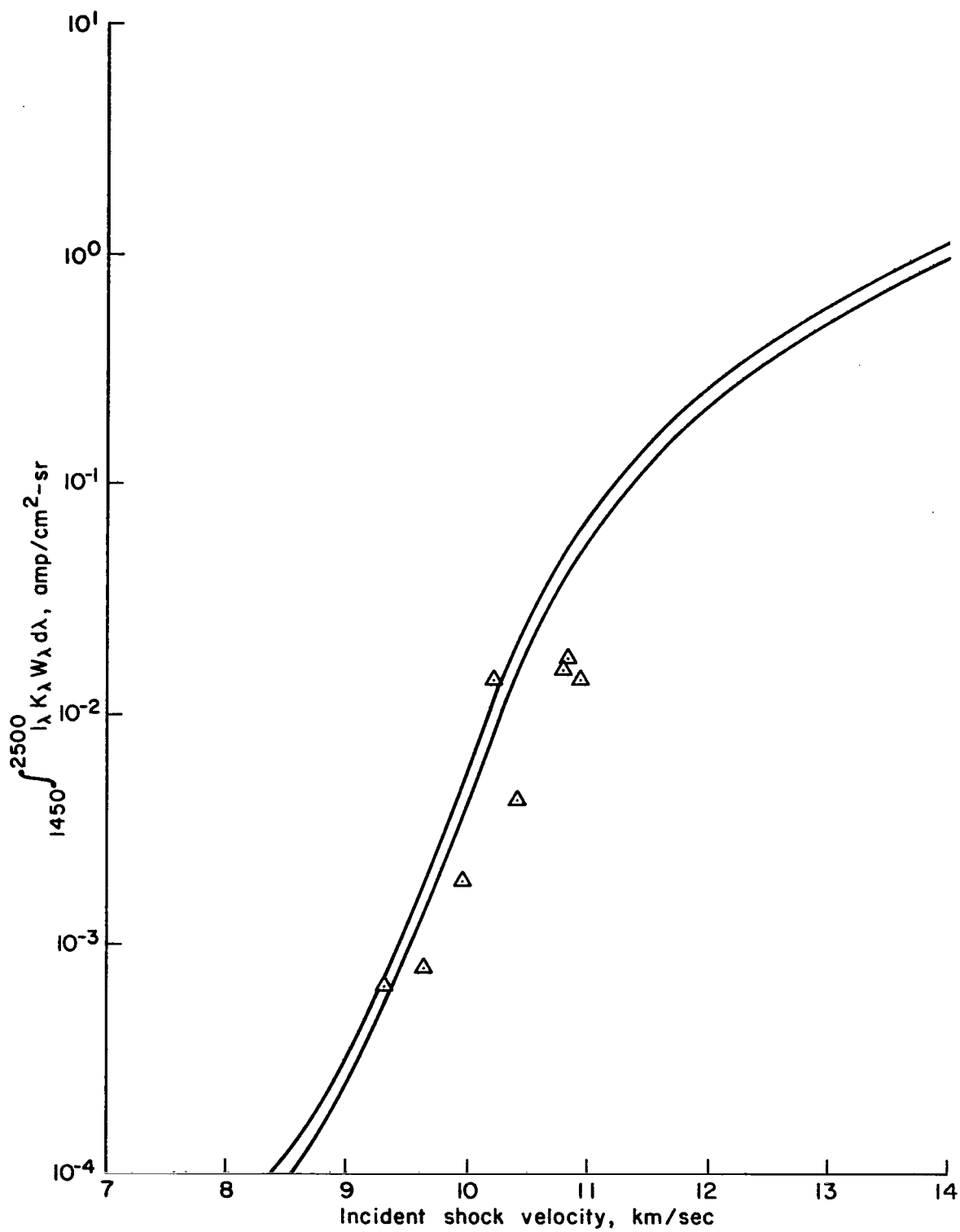
Figure 13.—Data obtained with second calcium fluoride plus sapphire window combination,
spectral range 1450-2500 Å.
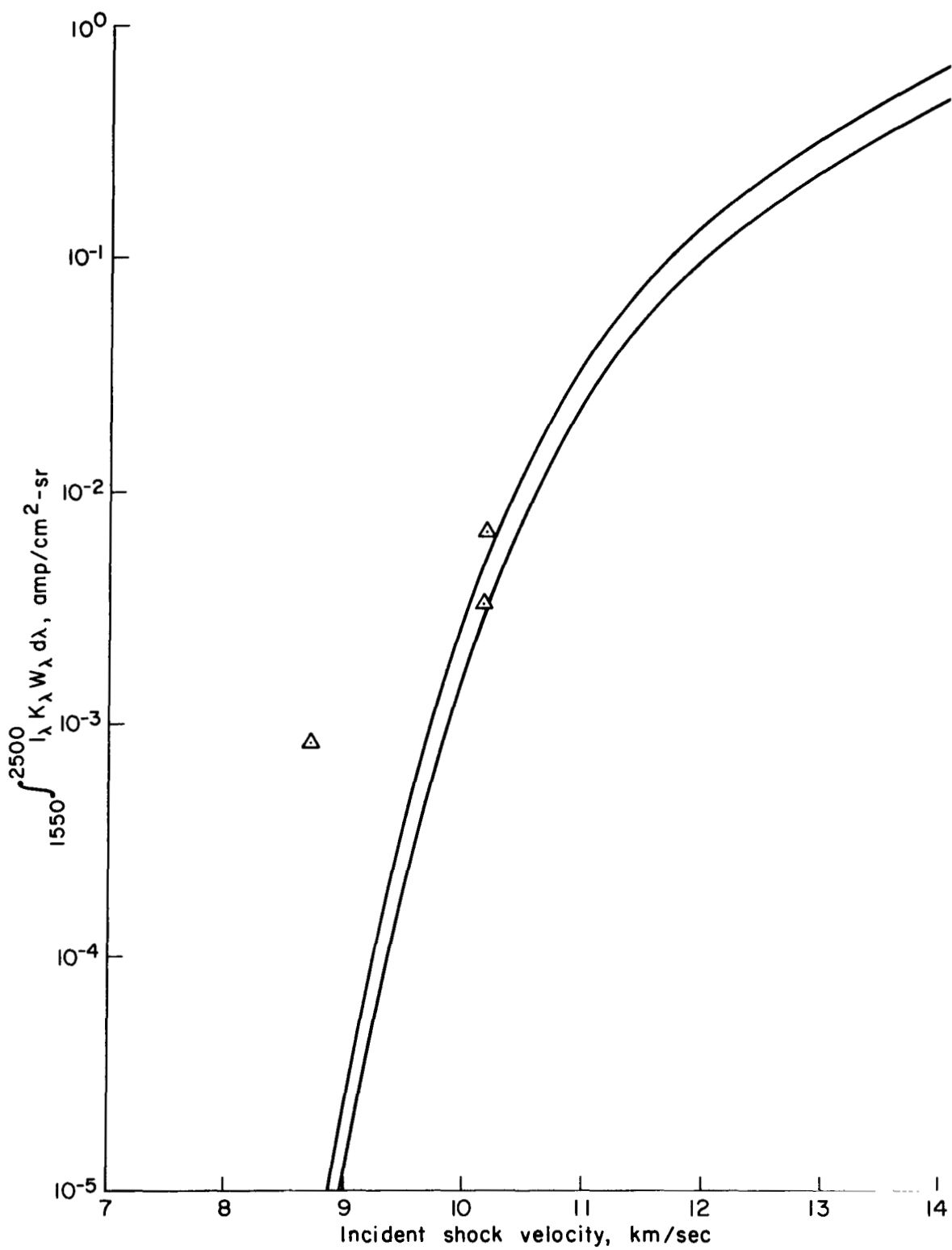
Figure 14.—Data obtained with suprasil (U.V. grade quartz) window, spectral range 1550-2500 Å.
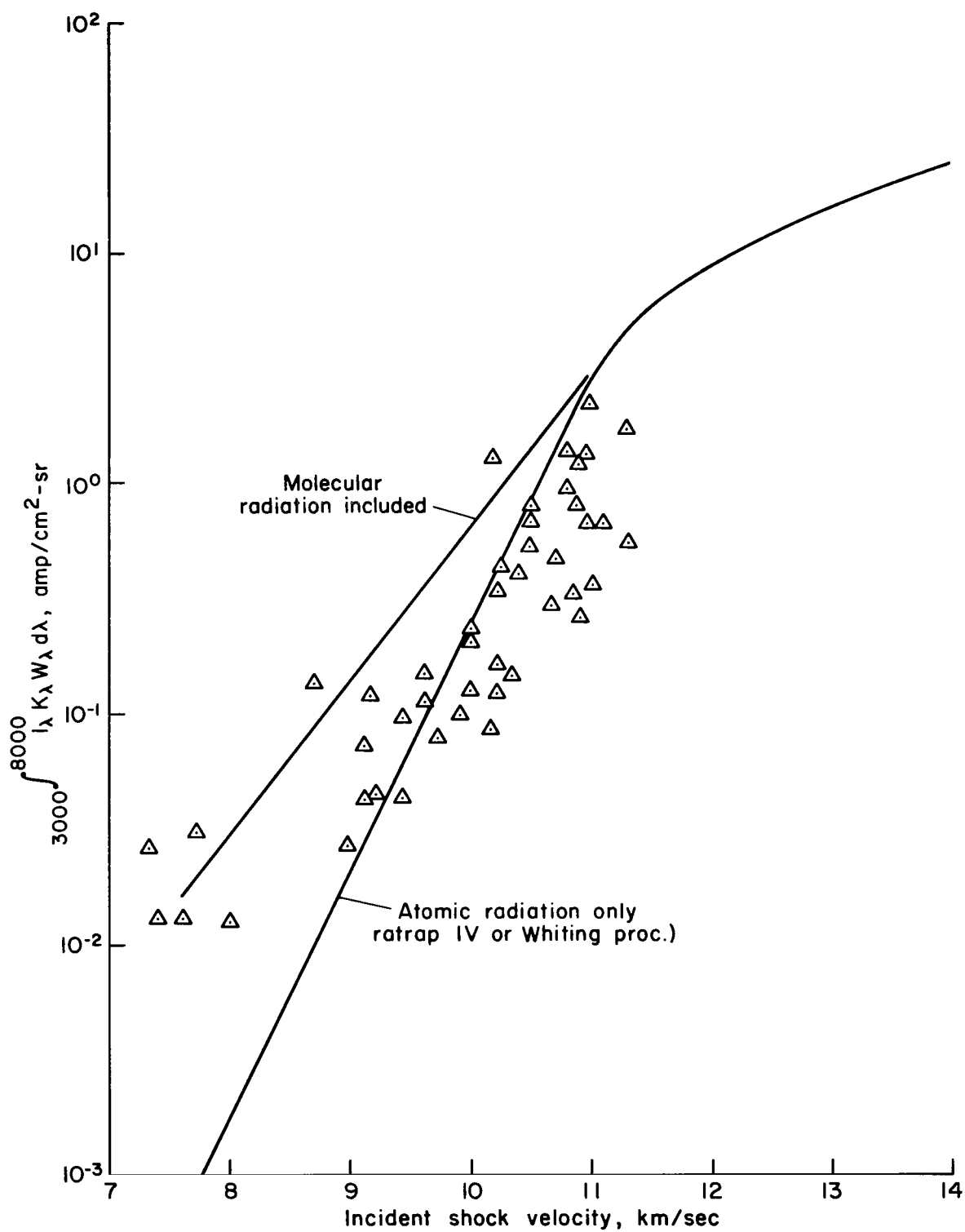
Figure 15.—Data obtained with visible detector system, spectral range 3000-8000 Å.
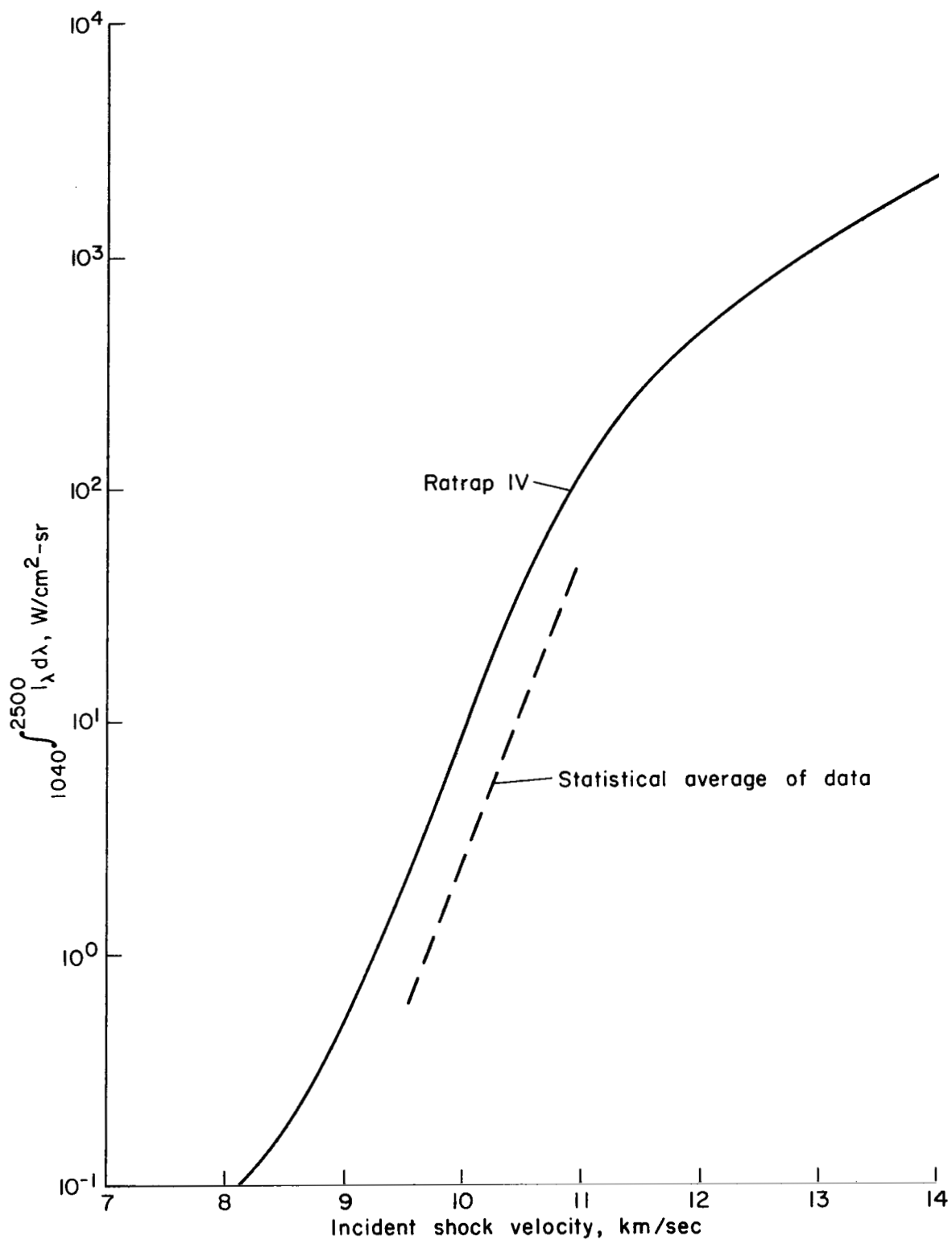
Figure 16.—Total power in spectral region between 1040 and 2500 Å.
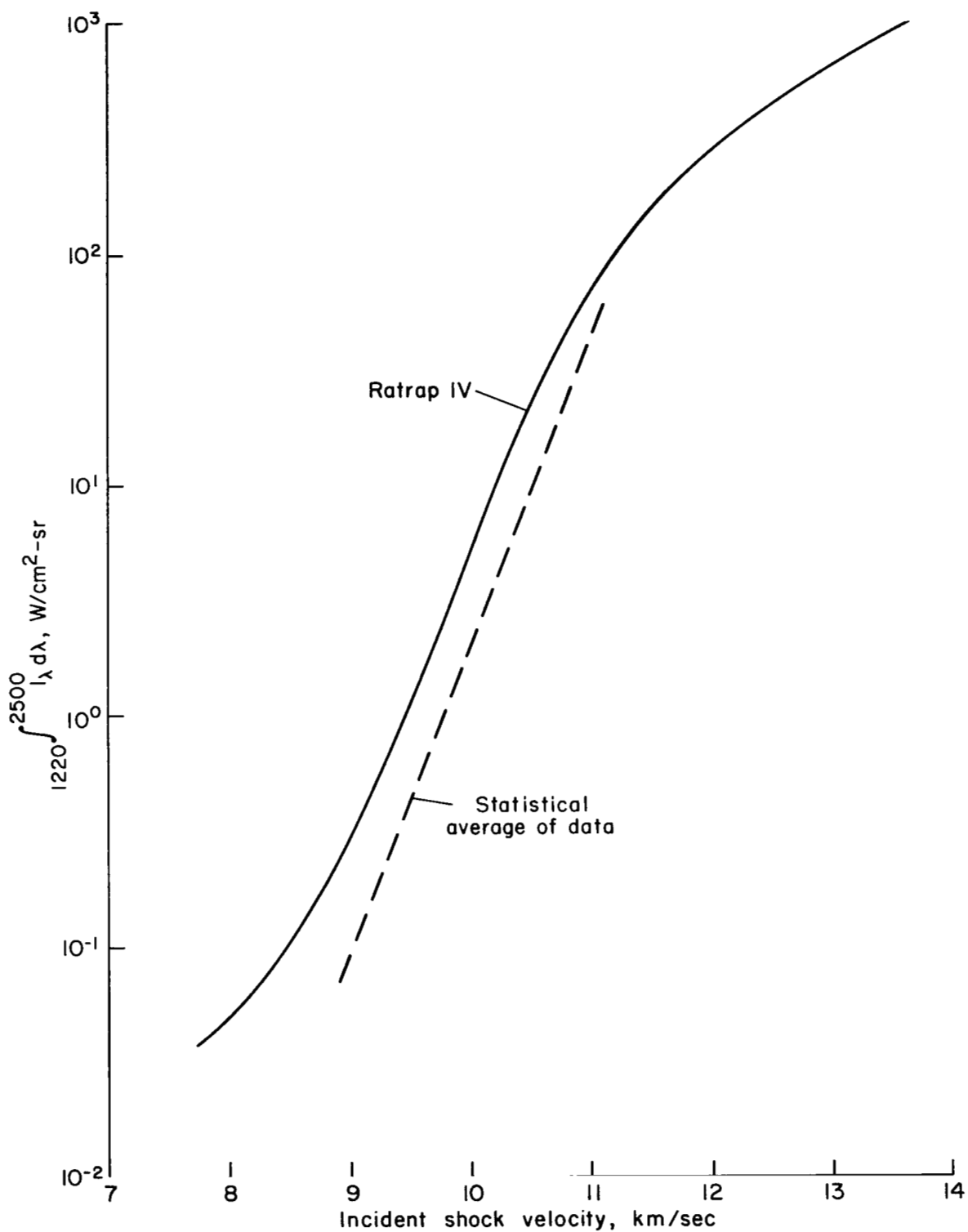
Figure 17.—Total power in spectral region between 1220 and 2500 Å.
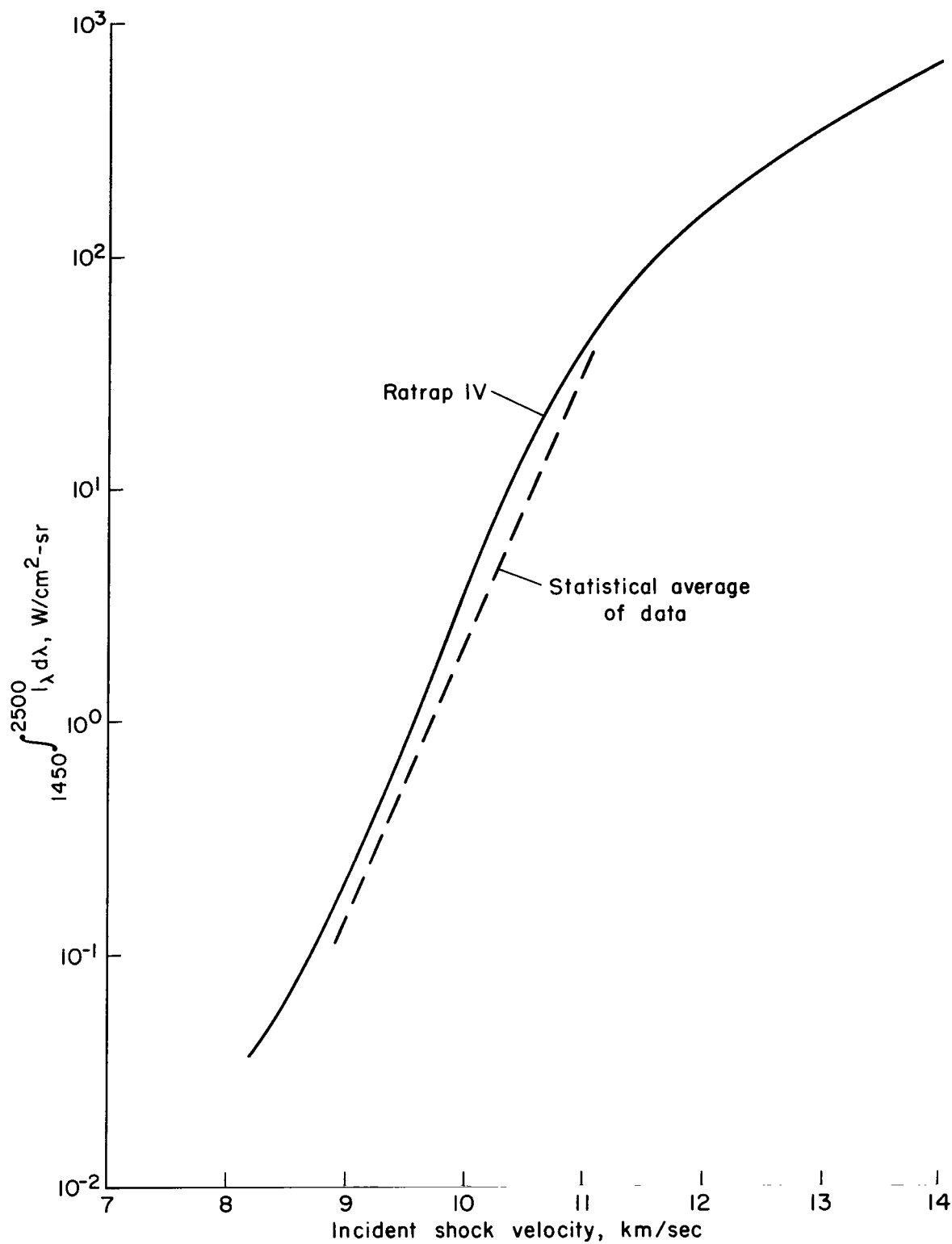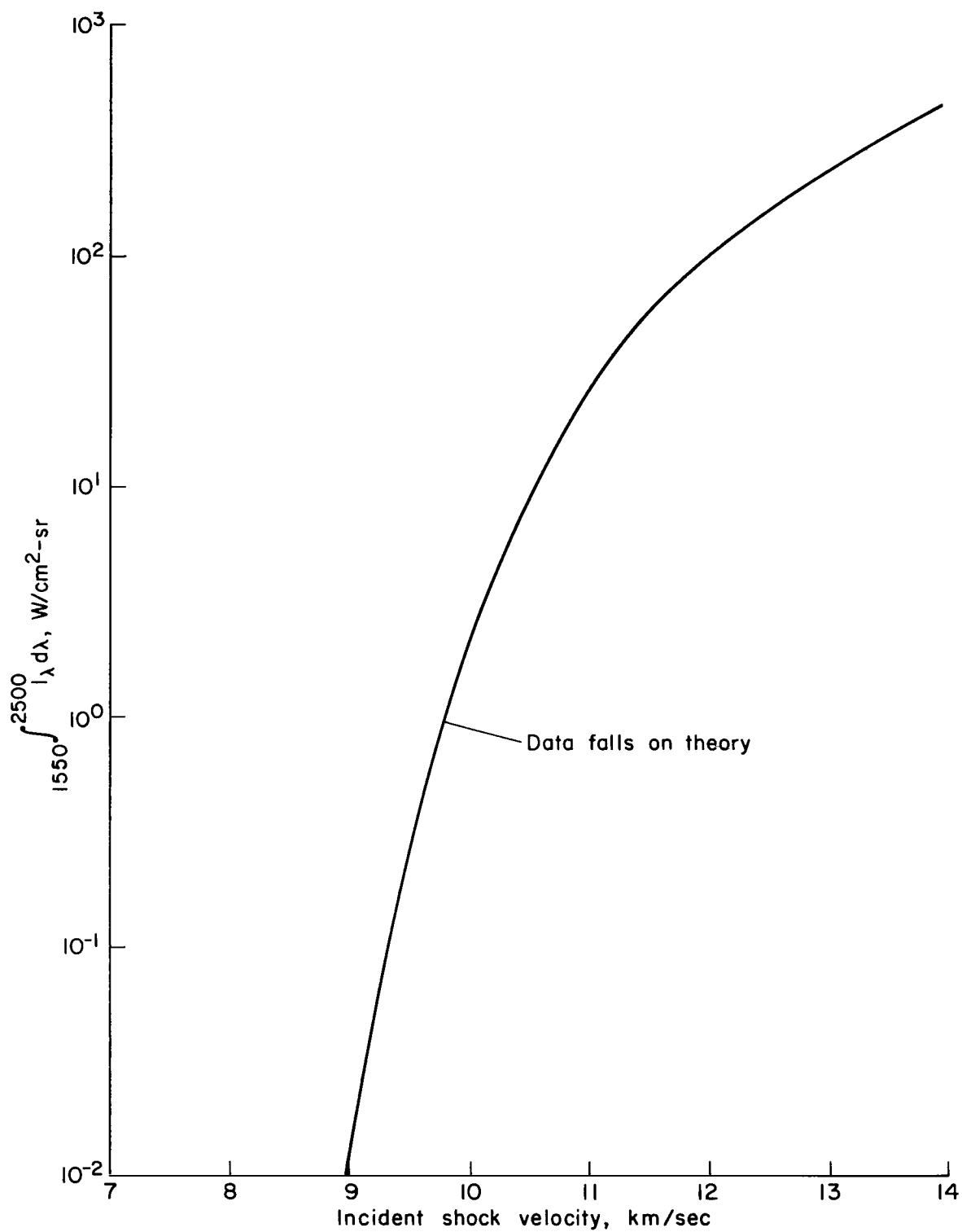
Figure 18.—Total power in spectral region between 1450 and 2500 Å.

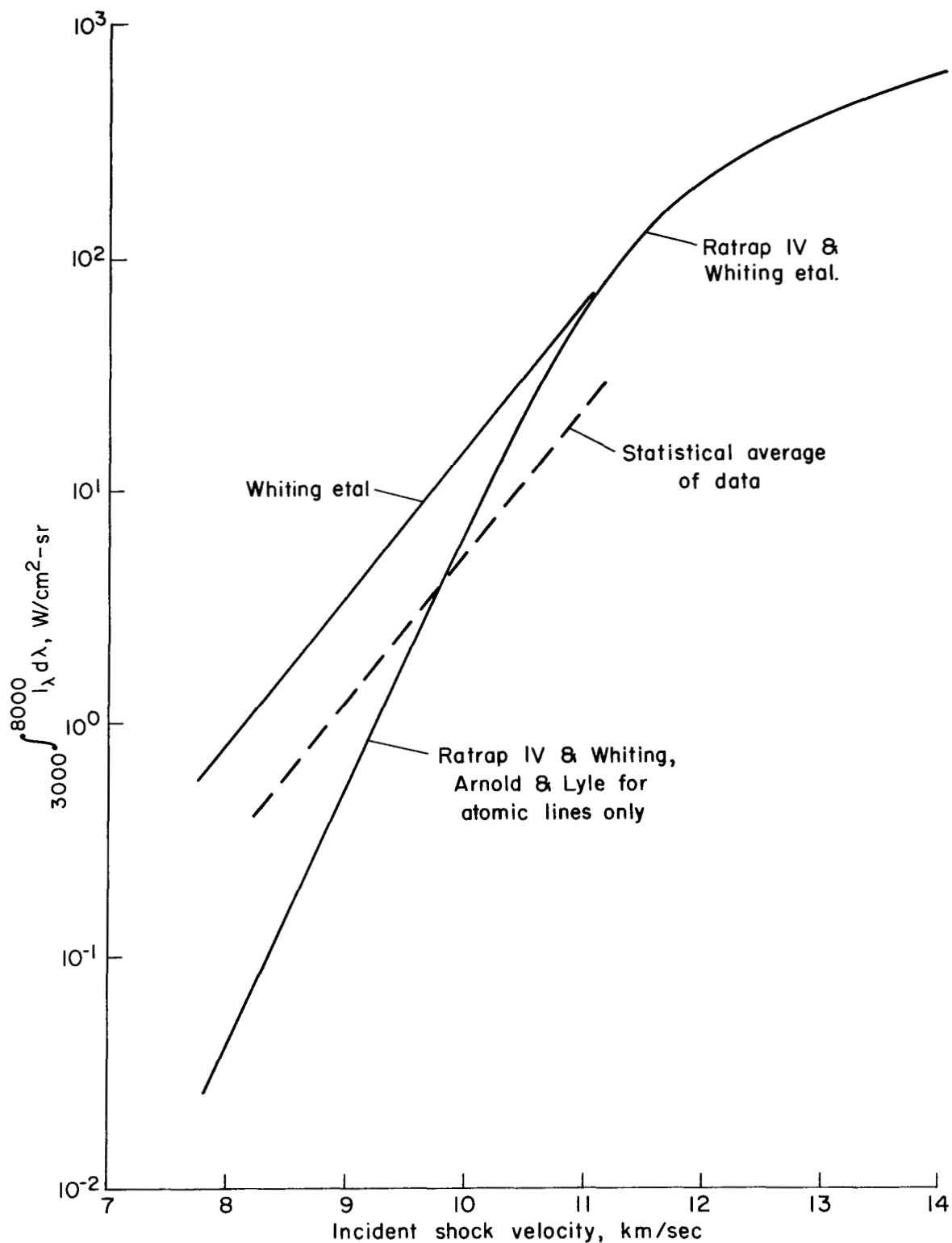Figure 19.—Total power in spectral region between 1550 and 2500 Å.

Figure 20.–Total power in spectral region between 3000 and 8000 Å.

"The aeronautical and space activities of the United States shall be conducted so as to contribute . . . to the expansion of human knowledge of phenomena in the atmosphere and space. The Administration shall provide for the widest practicable and appropriate dissemination of information concerning its activities and the results thereof."

— NATIONAL AERONAUTICS AND SPACE ACT OF 1958

NASA SCIENTIFIC AND TECHNICAL PUBLICATIONS

TECHNICAL REPORTS: Scientific and technical information considered important, complete, and a lasting contribution to existing knowledge.

TECHNICAL NOTES: Information less broad in scope but nevertheless of importance as a contribution to existing knowledge.

TECHNICAL MEMORANDUMS: Information receiving limited distribution because of preliminary data, security classification, or other reasons.

CONTRACTOR REPORTS: Scientific and technical information generated under a NASA contract or grant and considered an important contribution to existing knowledge.

TECHNICAL TRANSLATIONS: Information published in a foreign language considered to merit NASA distribution in English.

SPECIAL PUBLICATIONS: Information derived from or of value to NASA activities. Publications include conference proceedings, monographs, data compilations, handbooks, sourcebooks, and special bibliographies.

TECHNOLOGY UTILIZATION PUBLICATIONS: Information on technology used by NASA that may be of particular interest in commercial and other non-aerospace applications. Publications include Tech Briefs, Technology Utilization Reports and Technology Surveys.

Details on the availability of these publications may be obtained from:

SCIENTIFIC AND TECHNICAL INFORMATION OFFICE

NATIONAL AERONAUTICS AND SPACE ADMINISTRATION
Washington, D.C. 20546